

The recurrent nova U Scorpii – an evolutionary considerations

Marek J. Sarna¹, Ene Ergma² and Jelena Gerškevič^{2,1}

¹ N. Copernicus Astronomical Center, Polish Academy of Sciences, ul. Bartycka 18, 00-716 Warsaw, Poland

e-mail: sarna@camk.edu.pl; jelena@camk.edu.pl

² Physics Department, Tartu University, Ülikooli 18, 50510 Tartu, Estonia
e-mail: ene@physic.ut.ee; jelen_a@physic.ut.ee

Abstract

We perform evolutionary calculations of binary stars to find progenitors of systems with parameters similar to the recurrent nova U Sco. We show that a U Sco-type system may be formed starting with an initial binary system which has a low-mass carbon-oxygen white dwarf as an accretor. Since the evolutionary stage of the secondary is not well known, we calculate sequences with hydrogen-rich and helium-rich secondaries. The evolution of the binary may be divided into several observable stages as: classical nova, supersoft X-ray source with stable hydrogen shell burning, or strong wind phase. It culminates in the formation of a massive white dwarf near the Chandrasekhar mass limit. We follow the chemical evolution of the secondary as well as of the matter lost from the system, and we show that observed $^{12}\text{C}/^{13}\text{C}$ and N/C ratios may give some information about the nature of the binary.

1 Introduction

Recurrent novae are a small class of objects which bear many similarities to other cataclysmic variable systems. They experience recurrent outbursts at intervals of 10–80 yrs.

Recurrent novae have been proposed as possible progenitors of type Ia supernovae (Starrfield, Sparks & Truran 1985). Although they experience recurrent outbursts it is thought that the white dwarf mass would grow to finally exceed Chandrasekhar mass limit.

Webbink et al. (1987) discussed the nature of the recurrent novae, and they concluded that according to outburst mechanisms there are two subclasses of these systems: (a) powered by thermonuclear runaway on the surface of the white dwarf (e.g. U Sco), and (b) powered by the transfer of a burst of matter from the red giant to the main-sequence companion.

U Sco is one of the best observed recurrent novae. Historically, its outbursts were observed in 1863, 1906, 1917, 1936, 1979, 1987 and in 1999. Schaefer (2004) discovered on Harvard College Observatory archival photographs unknown eruption of the recurrent nova U Sco in 1917. Schaefer notes that U Sco has a fairly constant recurrent cycle of 8–12 yrs, with about 25% of the outbursts

being missed due to proximity to the sun (including potential missed outbursts around 1926 and 1957). Determinations of the system visual luminosity at maximum and minimum indicate a range $\Delta m_V \sim 9$. Schaefer (1990) and Schaefer & Ringwald (1995) observed eclipses of U Sco in the quiescent phase, and determined the orbital period $P_{\text{orb}}=1.23056$ d.

For the 1979 outburst, ejecta abundances have been estimated from optical and UV studies by Williams et al. (1981) and Barlow et al. (1981). They derived extremely helium rich ejecta $\text{He}/\text{H} \sim 2$ (by number), while the CNO abundance was solar with an enhanced N/C ratio. From analysis of the 1999 outburst, Anupama & Dewangan (2000) obtained an average helium abundance by number of $\text{He}/\text{H} \sim 0.4 \pm 0.06$, while Iijima (2002) 0.16 ± 0.02 . The estimated mass of the ejected shell for 1979 and 1999 outbursts is $\sim 10^{-7} M_{\odot}$ (Williams et al. 1981; Anupama & Dewangan 2000). Hachisu et al. (2000) and Matsumoto, Kato & Hachisu (2003) estimated the envelope mass at the optical maximum as being $\sim 3 \times 10^{-6} M_{\odot}$. If this is the present case, the mass accretion rate should be smaller than $\sim 2.5 \times 10^{-7} M_{\odot} \text{ yr}^{-1}$ in the quiescence between 1987 and 1999. Spectroscopically, U Sco shows very high ejection velocities of $(7.5-11) \times 10^3 \text{ km s}^{-1}$ (Williams et al. 1981; Munari et al. 2000). Latest determinations of the spectral type of the secondary indicate a K2 subgiant (Anupama & Dewangan 2000; Kahabka et al. 1999). According to Kahabka et al. (1999) the distance to U Sco is about 14 kpc.

Recently, the spectroscopic orbit of U Sco was determined by Thoroughgood et al. (2001). The radial velocity semiamplitudes for primary and secondary stars yield $M_{\text{wd}} = 1.55 \pm 0.24 M_{\odot}$ for the white dwarf and $M_2 = 0.88 \pm 0.17 M_{\odot}$ for a secondary star.

According to a model proposed by Kato (1996), supersoft X-ray emission should be observed about 10–60 days after the optical outburst. Indeed, BeppoSAX detected X-ray emission from U Sco at 0.2–20 keV just 19–20 days after the peak of its optical outburst in February 1999 (Kahabka et al. 1999). The fact that U Sco was detected as a supersoft X-ray source (SSS) is consistent with steady hydrogen shell burning on the surface of its white dwarf component.

In this paper we construct a grid of evolutionary sequences which may lead to formation of U Sco-like systems. In Section 2 we discuss the major phases of semidetached binary evolution. In Section 3 the evolutionary code is briefly described. Section 4 contains the results of the calculations. A general discussion and conclusions follow.

2 The major modes of semidetached binary evolution

We can identify three different modes of semidetached evolution of a close binary system with white dwarf as accretor:

- i) novae (nova outbursts);
- ii) stable hydrogen shell burning on a compact white dwarf; and
- iii) a strong, optically thick wind powered by steady hydrogen burning.

While calculating evolutionary models of binary stars, we must take into account mass transfer and associated physical mechanisms which lead to mass and angular momentum loss. We can express the change in the total orbital angular momentum (J) of a binary system as

$$\frac{\dot{J}}{J} = \frac{\dot{J}}{J}\bigg|_{\text{MSW}} + \frac{\dot{J}}{J}\bigg|_{\text{NOAML}} + \frac{\dot{J}}{J}\bigg|_{\text{FWIND}} + \frac{\dot{J}}{J}\bigg|_{\text{FAML}} \quad (1)$$

where the terms on the right hand side are due to: magnetic stellar wind braking (MSW); nova outburst

angular momentum loss, which describes the loss of angular momentum from the system due to non-conservative evolution (NOAML); optically thick wind angular momentum loss from the white dwarf during stable hydrogen shell burning (FWIND); and frictional angular momentum loss in a strong optically thick wind (FAML).

To account for magnetic stellar wind braking, we use the Skumanich (1972) ‘law’,

$$\left. \frac{J}{J} \right|_{\text{MSW}} = - \left\{ (5.0 \times 10^{-29}) (2\pi)^{\frac{10}{3}} \text{G}^{-\frac{2}{3}} \right\} \left(\frac{k_2}{\lambda} \right)^2 \frac{M_{\text{tot}}^{\frac{1}{3}} R_{\text{sg}}^4}{M_{\text{wd}}} P_{\text{orb}}^{-\frac{10}{3}} \quad (2)$$

where M_{wd} and M_{tot} denote, respectively, the mass of the white dwarf primary and the total mass of the system; R_{sg} is the radius of the secondary star; k_2 is the radius of gyration of the secondary star, $k_2^2 = 0.1$ (Webbink 1976) and λ characterizes the effectiveness of dynamo action in the stellar convective zone. Values of $\lambda = 0.73$ (Skumanich 1972) or $\lambda = 1.78$ (Smith 1979) can be found in the literature; however, we use a value of $\lambda = 1$ according to Ergma & Sarna (2000) model calculations (the best fit to the observed orbital decay of the PSR B1744–24A). We assume that MSW losses are present in all three modes of evolution identified here.

2.1 Novae

In novae, angular momentum loss accompanies mass loss due to the nova outbursts.

2.1.1 Angular momentum loss associated with nova outbursts

To take account of the angular momentum loss accompanying mass loss in nova outbursts, we use a formula based on that used to calculate angular momentum loss via a stellar wind (Paczynski & Ziółkowski 1967; Ziółkowski 1985 and De Greve 1993),

$$\left. \frac{J}{J} \right|_{\text{NOAML}} = f_1 f_2 \frac{M_{\text{wd}} \dot{M}_{\text{sg}}}{M_{\text{sg}} M_{\text{tot}}}, \quad \text{where } \dot{M} = f_1 \dot{M}_{\text{sg}}. \quad (3)$$

Here, f_1 is the ratio of the mass ejected by the white dwarf to that accreted by the white dwarf,

$$f_1 = \frac{\Delta M_{\text{ej}}}{\Delta M_{\text{acc}}}, \quad (4)$$

where ΔM_{acc} and ΔM_{ej} are the amounts of matter transferred from the secondary to the white dwarf and ejected in a nova outburst, during one nova cycle, respectively. The parameter f_2 described the effectiveness of angular momentum loss during mass transfer (Sarna & De Greve 1994, 1996); M_{sg} denotes the mass of the subgiant secondary; \dot{M}_{sg} is the rate of mass loss from the secondary ($-\dot{M}_{\text{sg}}$ is equivalent to the mass transfer rate). We employ the code developed by Marks & Sarna (1998) (hereafter MS98), which utilizes the results of the theoretical novae calculations of Prialnik & Kovetz (1995) and Kovetz & Prialnik (1997) (hereafter PK95 and KP97). Using this data, we are able to compute the value of f_1 , which we have previously had to assume as free parameter (Sarna, Marks & Smith 1996). By interpolation from the data of PK95 and KP97, at each time step, we use the

white dwarf mass and the mass transfer rate to determine the nova characteristics: f_1 , amplitude of the outburst (A), recurrence period (P_{rec}), and chemical composition of the ejected material (for more details see MS98).

We take $f_2 = 1.0$, which is typical for a stellar wind. Livio & Pringle (1998) proposed a model in which the accreted angular momentum is removed from the system during nova outbursts, as previously suggested by Marks, Sarna & Prialnik (1997). Equation (3) is in quantitative agreement with these estimations.

As discussed by MS98, angular momentum loss rates from nova outbursts are comparable with MSW losses. As an illustration, we can estimate the characteristic time scales [$\tau = (J/J)^{-1}$] for both mechanisms. We assume a binary system in the same evolutionary stage as U Sco, with components of 0.94 and 1.3 M_{\odot} and orbital period 1.23 d. The secondary has a radius 2.22 R_{\odot} ; $f_1 = 0.92$ and the mass transfer rate from the secondary to white dwarf is $3.3 \times 10^{-8} M_{\odot} \text{ yr}^{-1}$. We obtain $\tau_{\text{MSW}} \sim 1.5 \times 10^{16} \text{ s}$ and $\tau_{\text{NOAML}} \sim 1.7 \times 10^{15} \text{ s}$, i.e., angular momentum losses associated with nova outbursts is about an order of magnitude greater than those from the magnetic stellar wind.

2.1.2 Accretion of material ejected during nova outbursts

To calculate the re-accretion by the secondary of material ejected during nova outbursts, we assume that the mass of the material re-accreted ($M_{\text{re-acc}}$) is proportional to the mass of the material ejected by the white dwarf, such that

$$M_{\text{re-acc}} = \left(\frac{R_{\text{sg}}}{2a} \right)^2 \Delta M_{\text{ej}} . \quad (5)$$

The constant of proportionality is the ratio of the cross-section area of the secondary star to the area of a sphere at radius a from the white dwarf. We base this formula on the assumption that nova ejections are spherically symmetric, with ejection velocities large compared with the orbital velocity of the companion.

During nova outbursts, matter which is re-accreted by the secondary changes significantly its chemical composition.

2.2 Stable hydrogen shell burning

We assume that during stable hydrogen shell burning, only angular momentum losses due to the magnetic stellar wind will be important.

2.3 Strong optically thick wind

In this phase, two more processes change the total angular momentum and mass of the system: a strong optically thick wind, and frictional deposition of orbital energy into that wind.

2.3.1 Loss of angular momentum due to an optically thick wind

If we consider a carbon-oxygen (C-O) white dwarf accreting matter from a companion with solar composition, there exists a critical accretion rate above which the excess material is blown off in a strong wind. Hachisu et al. (1996) show that because wind velocity is about 10 times higher

than orbital velocity, the wind has the same specific angular momentum as the white dwarf. The corresponding loss rate is

$$\left. \frac{j}{J} \right|_{\text{FWIND}} = \frac{q}{(1+q)} \frac{\dot{M}_{\text{wind}}}{M_{\text{wd}}}, \quad (6)$$

where $q = M_{\text{sg}}/M_{\text{wd}}$ is the mass ratio and \dot{M}_{wind} is the mass loss rate from the system. This mechanism will be very effective during strong optically thick wind. Note also that during the wind phase, the relatively small specific angular momentum content of the wind tends to stabilize mass transfer (Hachisu et al. 1996; Li & van den Heuvel 1997).

2.3.2 Frictional angular momentum loss

During an optically thick wind phase, the secondary star effectively orbits within the dense wind. Due to the frictional deposition of orbital energy into the wind, the separation of the components will be decreased.

Livio, Govarie & Ritter (1991) estimated the change in the orbital angular momentum brought about by frictional angular momentum loss,

$$\left. \frac{j}{J} \right|_{\text{FAML}} = \frac{1}{4} (1+q) \frac{(1+U^2)^{\frac{1}{2}}}{U} \left(\frac{R_{\text{sg}}}{a} \right)^2 \frac{\dot{M}_{\text{wind}}}{M_{\text{sg}}}, \quad (7)$$

where $U \equiv (v_{\text{exp}}/v_{\text{orb}})$ is the ratio of the expansion velocity of the envelope at the position of the secondary to the orbital velocity of the secondary in the primary's frame of reference, a is the separation of the system, and \dot{M}_{wind} is the rate of mass flow past the secondary (Warner 1995). Hachisu, Kato & Nomoto (1996) estimated that $v_{\text{exp}}/v_{\text{orb}} \sim 10$.

2.3.3 Re-accretion of material from strong wind

We define two critical mass accretion rates onto white dwarf. First (Warner 1995):

$$\dot{M}_{\text{cr},1} = 2.3 \times 10^{-7} (M_{\text{wd}} - 0.19)^{3/2} [\text{M}_{\odot} \text{ yr}^{-1}], \quad (8)$$

where $\dot{M}_{\text{cr},1}$ is the critical accretion rate above which hydrogen shell burning is stable. Second (Nomoto, Nariai & Sugimoto 1979; Hachisu et al. 1996):

$$\dot{M}_{\text{cr},2} = 9.0 \times 10^{-7} (M_{\text{wd}} - 0.5) [\text{M}_{\odot} \text{ yr}^{-1}], \quad (9)$$

where $\dot{M}_{\text{cr},2}$ is the critical accretion rate above which a strong wind occurs. In the latter case, the hydrogen is burning into helium at a rate close to $\dot{M}_{\text{cr},2}$, with the excess material being blown off by the wind at the rate:

$$\dot{M}_{\text{wind}} = \dot{M}_{\text{sg}} - \dot{M}_{\text{cr},2}. \quad (10)$$

To calculate re-accretion of material from the wind by the secondary, we assume that, as in eq. (5), the mass of re-accreted material is proportional to the mass loss rate from the white dwarf (\dot{M}_{wind}).

We may estimate the characteristic time scales for each of angular momentum loss mechanisms during a strong wind phase. We find, for example, that such a wind occurs for a binary system

with component masses 1.57 and $0.95 M_{\odot}$, and an orbital period of 1.1 d. In such a system, the secondary has a radius of $\sim 2.6 R_{\odot}$, $f_1=0.4$, the mass transfer rate from the secondary to white dwarf is $1.05 \times 10^{-6} M_{\odot} \text{ yr}^{-1}$, $\dot{M}_{\text{wind}} = 4 \times 10^{-7} M_{\odot} \text{ yr}^{-1}$, and $U=10$. The characteristic time scales are then: $\tau_{\text{MSW}} \sim 5 \times 10^{18} \text{ s}$, $\tau_{\text{FAML}} \sim 3 \times 10^{15} \text{ s}$ and $\tau_{\text{FWIND}} \sim 5 \times 10^{14} \text{ s}$.

3 The evolutionary code

Models of secondary stars filling their Roche lobes were computed using a standard stellar evolution code based on the Henyey-type code of Paczyński (1970), which has been adapted to low-mass stars (as described in detail in MS98). We use the Eggleton (1983) formula to calculate the size of the secondary's Roche lobe.

For radiative transport, we use the opacity tables of Iglesias & Rogers (1996). Where the Iglesias & Rogers (1996) tables are incomplete, we have filled the gaps using the opacity tables of Huebner et al. (1977). For temperatures lower than 6000 K , we use the opacities given by Alexander & Ferguson (1994) and Alexander (private communication).

3.1 Nuclear network

Our nuclear reaction network is based on that of Kudryashov & Ergma (1980), who included the reactions of the CNO tri-cycle in their calculations of hydrogen and helium burning in the envelope of an accreting neutron star. We have included the reactions of the proton-proton (PP) chain. Hence we are able to follow the evolution of the elements: ^1H , ^3He , ^4He , ^7Be , ^{12}C , ^{13}C , ^{13}N , ^{14}N , ^{15}N , ^{14}O , ^{15}O , ^{16}O , ^{17}O and ^{17}F . We assume that the abundances of ^{18}O and ^{20}Ne stay constant throughout the evolution. We use the reaction rates of: Fowler, Caughlan & Zimmerman (1967, 1975), Harris et al. (1983), Caughlan et al. (1985), Caughlan & Fowler (1988), Bahcall & Ulrich (1988), Bahcall & Pinsonneault (1992), Bahcall, Pinsonneault & Wesserburg (1995) and Pols et al. (1995).

3.2 The role of unstable helium burning

In recent years several papers concerning unstable helium burning in accreting white dwarfs have been published. Cassini, Iben & Tornambe (1998) investigated accretion onto cool C-O white dwarfs of masses 0.5 and $0.8 M_{\odot}$. They considered broad range of mass accretion rates from 10^{-8} to $10^{-6} M_{\odot} \text{ yr}^{-1}$. They found that even in the case when hydrogen burns at the same rate at which it is accreting, helium flash leads to envelope expansion. The expanded envelope, due to interaction with the companion star is lost from the system. The net result is that the mass of the accreting white dwarf decreases.

Kato & Hachisu (1999) proposed that if an optically thick wind occurs during helium shell flashes, due to its high velocity ($\sim 1000 \text{ km s}^{-1}$) the wind leaves the system without interaction with the companion star. They found that at a relatively high accretion rate, the mass accumulation efficiency is large enough for the white dwarf to grow above the Chandrasekhar mass limit. However, it is important to note that they considered an initially relatively massive ($1.3 M_{\odot}$) white dwarf, and neglected restriction by hydrogen shell burning of the maximum accretion rate (see formula (9)). Because of these approximations, the mass accumulation ratio, $1 - f_1$, never equals unity.

Table 1 Initial parameters of computed sequences

model	M_{sg} [M_{\odot}]	M_{wd} [M_{\odot}]	$P_1(\text{RLOF})$ [d]	X	Z
A	1.4	0.70	1.34	0.68	0.02
B	1.7	0.85	1.61	0.68	0.02
C	1.4	0.70	1.26	0.50	0.02
D	1.7	0.85	1.24	0.50	0.02

Langer et al. (2000) considered the evolution of main sequence star + white dwarf binary systems towards type Ia supernovae. They assumed that above some critical accretion rate ($10^{-8} M_{\odot} \text{ yr}^{-1}$ — for Population I) helium burning proceeds such that violent nova flashes and consequent mass ejection from the white dwarf are avoided.

In our calculations, mass loss due to unstable helium burning has been neglected. So that the masses of white dwarfs we obtain are overestimated.

4 Results of calculations

4.1 The grid of models

To understand the evolution of close binary system consisting of a C-O or NeMgO white dwarfs and near-main-sequence or helium-rich stars, we computed various evolutionary sequences for three chemical compositions (Population II — $X=0.756$, $Z=0.001$; Population I — $X=0.68$, $Z=0.02$; and helium rich — $X=0.5$, $Z=0.02$), for four initial mass ratios $q_i = M_{\text{sg},i}/M_{\text{wd},i} = 1.5, 2.0, 2.5, 3.0$ and five white dwarf masses: $0.7, 0.85, 1.0, 1.15, 1.3 M_{\odot}$. For each system three different evolutionary stages for secondary star are followed: i) the secondary fills its Roche lobe as a M-S star with central hydrogen content $X_c \sim 0.4$; ii) the secondary fills its Roche lobe as a terminal M-S star with small helium core $M_{\text{HeCore}} \sim 0.01 M_{\odot}$; and iii) the secondary fills Roche lobe upon reaching helium core more $M_{\text{HeCore}} \sim 0.1 M_{\odot}$ (Sarna, Ergma & Gerškevičs, in preparation). We found that only a few evolutionary sequences are able to produce system parameters similar to U Sco. Since the evolutionary stage of the secondary (hydrogen- or helium-rich) is not observationally well-determined, we selected from our grid of models four different sequences with hydrogen and helium rich secondaries. Initial parameters of the sequences are presented in Table 1.

The sequences C and D represent the helium rich channel proposed by Hachisu et al. (1999). In Table 2 results for computed sequences are shown. The masses of the subgiant and the white dwarf are given at the moment when orbital period of the system is equal to 1.23 d. The effective temperature and luminosity are for the subgiant star.

An extended grid of multi-cycle nova evolution models by Prialnik & Kovetz (1995) allows to find entire range of observed nova characteristics including recurrent and symbiotic novae. In Fig. 1, three characteristic lines are drawn, according to the PK95 calculations and their classification scheme. Fast, slow and symbiotic novae are located below line 1 (we used the classification scheme of PK95). Between lines 1 and 2, recurrent novae with recurrence periods longer than 10 yr but shorter than 100 yr are located. Above line 2 but below line 3, the mass accretion rate onto the white dwarf is higher than $\dot{M}_{\text{cr},1}$ and nova outbursts do not occur — hydrogen burning is stable. Above line

Table 2 Results for computed sequences

model	M_{sg} [M_{\odot}]	M_{wd} [M_{\odot}]	$\log T_{\text{eff}}$ [K]	$\log L/L_{\odot}$	\dot{M}_{sg} [$M_{\odot} \text{ yr}^{-1}$]
A	0.545	0.983	3.669	0.153	2.02×10^{-8}
B	0.936	1.304	3.693	0.416	3.58×10^{-8}
C	0.581	1.263	3.719	0.370	4.07×10^{-8}
D	1.696	0.852	3.957	1.707	1.14×10^{-7}

Table 3 Time-scales for evolutionary phases

model	Δt_{n1}	Δt_{s1}	Δt_{w}	Δt_{s2}	Δt_{rn}	Δt_{n2}
	[$\log(\Delta t/\text{yr})$]					
A	4.00	6.57	–	–	–	8.17
B	5.97	6.46	–	–	7.51	6.86
C	4.76	5.41	5.39	6.17	7.17	6.72
D	4.89	5.02	5.60	5.58	–	–

3, the stable hydrogen burning is accompanied by a strong optically thick wind. According to our calculations, all models go first through an short nova phase (n1). After that, all systems enter into the first stable hydrogen shell burning stage (s1). Sequences A and B do not exhibit a wind phase. After the stable burning stage, system A evolves into second nova phase (n2), while system B evolves into a recurrent nova phase. Sequences C and D have a wind phase (w) and a second stable hydrogen shell burning stage (s2). After the second stable hydrogen burning stage, sequence C evolves through recurrent novae phase (rn). Sequence D avoids a second nova phase. For this system, the white dwarf mass exceeds Chandrasekhar limit during stable hydrogen burning, and a supernova explosion may occur. In Table 3 the duration of each phase is shown. The duration of the stable hydrogen burning and wind phases varies among different sequences from several hundred thousand to several million years.

We infer that sequences B (hydrogen-rich) and C (helium-rich) may evolve into systems like U Sco. After stable hydrogen burning both sequences enter into a recurrent nova phase (Fig.1).

For the same two evolutionary sequences, in Fig. 2 we present evolution of the orbital period P_{orb} versus mass of the subgiant M_{sg} (Fig. 2a) and mass of the white dwarf M_{wd} (Fig. 2b). From our calculations we find that both systems (B and C) evolve through the orbital period $P_{\text{orb}} = 1.23$ d twice. During the first crossing of $P_{\text{orb}} = 1.23$ d line, the luminosity of the secondary is too high ($\log L/L_{\odot} \sim 0.9$ and 1.35 for sequences B and C, respectively) and it does not fit the observed absolute magnitude $M_V = +3.8$ of U Sco. During the second crossing, we find from the grid of nova models (PK95 and KP97) outburst amplitudes $A = 7.6$ mag and recurrence periods P_{rec} of 23 and 54 yrs, respectively, for sequences B and C. The mean recurrence interval implied by known outbursts is $P_{\text{rec}} = 13$ yrs (excluding outburst in 1863). Therefore, we conclude that sequence B provides the best fit to the observed parameters of U Sco.

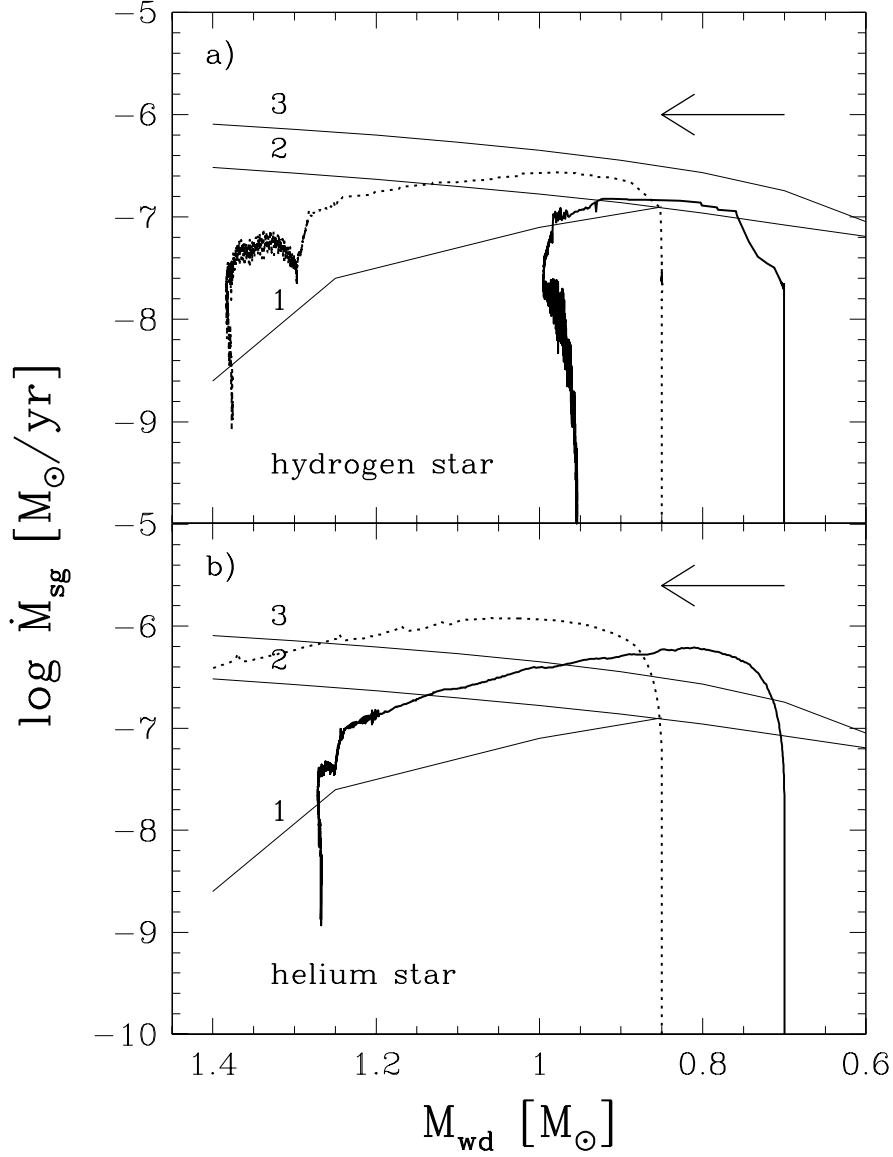


Figure 1: The evolution of the mass transfer rate versus white dwarf mass: (a) for a hydrogen-rich donor: sequence A (solid line) and sequence B (dashed line) from Table 1; (b) for helium-rich donor: sequence C (solid line) and sequence D (dashed line), also from Table 1. The lines marked 1, 2 and 3 show lower boundaries for recurrent novae, stable hydrogen burning and strong wind regions, respectively. The region bounded by lines 1 and 2 shows the recurrent nova phase. The arrows show the direction of evolution.

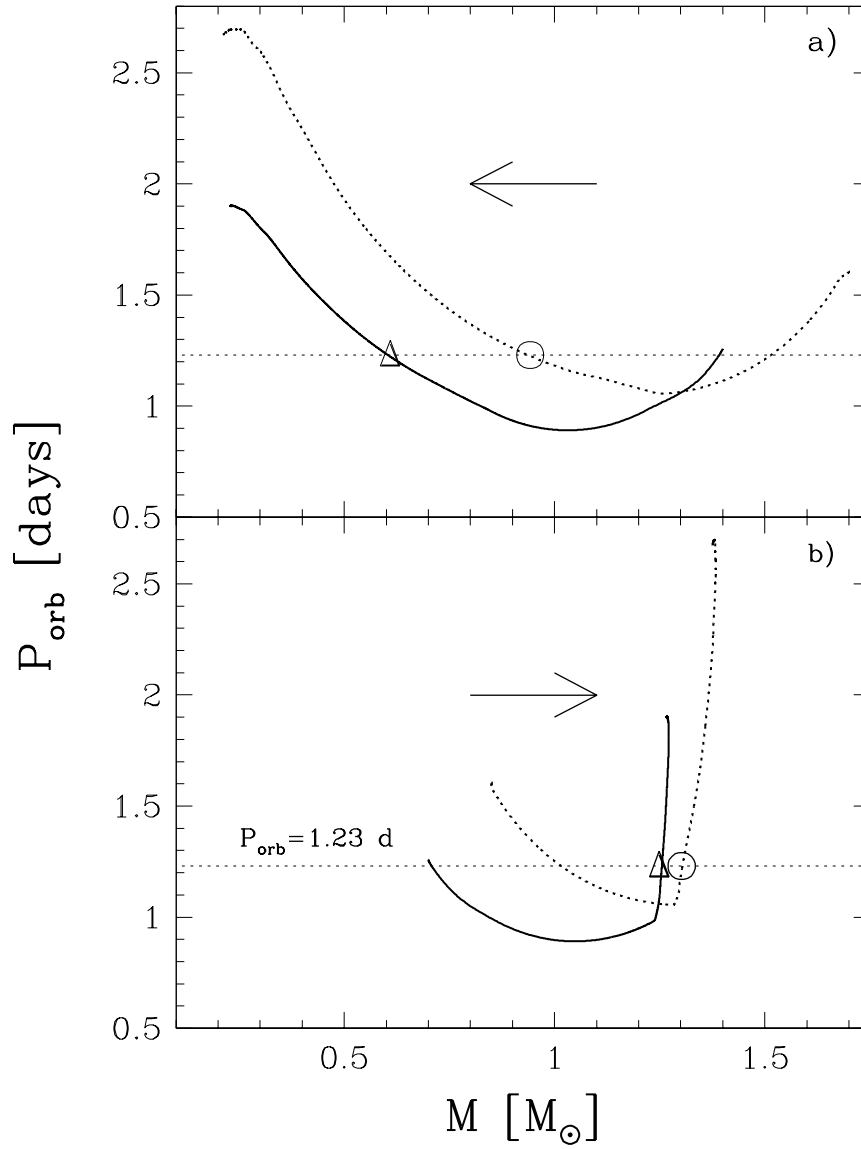


Figure 2: The evolution of the orbital period of the system as a function (a) of the subgiant mass M_{sg} : solid line — sequence C, dashed line — sequence B, and (b) of the white dwarf mass M_{wd} : solid line — sequence C, dashed line — sequence B. Horizontal thin dashed lines mark the orbital period of U Sco. Open circles mark positions of subgiant and white dwarf at this period for sequence B, open triangles for sequence C. The arrows show the direction of evolution.

Table 4 Chemical compositions (by mass) for sequences B and C at $P_{\text{orb}} = 1.23$ d.

model	^{12}C [$\times 10^{-3}$]	^{13}C [$\times 10^{-4}$]	^{14}N [$\times 10^{-3}$]	^{15}N [$\times 10^{-7}$]	^{16}O [$\times 10^{-3}$]	^{17}O [$\times 10^{-5}$]	$^{12}\text{C}/^{13}\text{C}$	N/C
B subgiant	1.41	3.05	3.16	5.64	9.77	0.58	4.6	1.8
B ejecta	2.81	11.51	42.06	251.60	1.77	200.00	2.4	10.6
C subgiant	0.31	1.07	4.69	2.91	9.77	1.10	2.9	11.3
C ejecta	1.93	7.10	35.89	94.82	3.82	51.75	2.7	13.6

4.2 Chemical composition of the subgiant and ejected matter

From the grid of models calculated by PK95 and KP97, we can interpolate the chemical composition of each model during its nova phase. In Table 4, the isotopic compositions in the envelope of the subgiant and in the ejected matter are shown (at $P_{\text{orb}} = 1.23$ d) for the two sequences B and C.

If we compare the helium-rich model C with the hydrogen-rich model B, we see that at $P_{\text{orb}} = 1.23$ d the N/C ratio in the envelope of the subgiant is higher for the helium-rich model, but the isotopic ratio $^{12}\text{C}/^{13}\text{C}$ is higher for the hydrogen-rich model. In the ejected matter, both ratios are similar for models B and C.

Our calculations show that as these models evolve, the He/H ratio of the matter lost from the system changes from 0.56 to 1.26. For sequences B and C, at $P_{\text{orb}} = 1.23$ d the He/H ratio is 0.75 and 0.65, respectively, *i.e.*, within the limits (0.4 – 2) obtained from observation (Anupama & Dewangan 2000, Williams et al. 1981).

Figs. 3 and 4 show the evolution of the abundances by mass of helium, hydrogen, carbon, nitrogen and oxygen of the subgiant envelope and ejected matter. The vertical thin dashed lines show the place where the orbital period is equal to 1.23 d. During stable hydrogen shell burning phases, no loss of matter from the system occurs. These phases are marked in Fig. 4 by setting $\log X_i = 0$.

5 Observational tests

Chemical composition and isotopic analysis may give more information about the evolutionary stage of U Sco. Unfortunately, the subgiant component in U Sco is too faint for infrared spectroscopic observations of CO bands in order to determine the $^{12}\text{C}/^{13}\text{C}$ ratio. However, we think that blue and red domain spectra of U Sco could show some absorption structure in the region of 4216Å and 7920Å in the CN sequence, similar to that observed in DQ Her (Chanan, Nelson & Margon 1978, Schneider & Greenstein 1979, Willimas 1983, Bauschlicher, Langhoff & Taylor 1988). Analysis of the blue region of the spectra is more complicated because the structure of the CN violet system can be affected by absorption features from the disc. However, we suggest that since the matter in the accretion disc reflects the chemical composition of the subgiant star, analysis of the disc will provide the information we need if we use observations made during the quiescent phase. We suggest that the red CN band is more useful for observations. We propose to observe spectral region near 7920–7940Å to identify two ^{13}CN lines at 7921.13Å and 7935.67Å which are important for both $^{12}\text{C}/^{13}\text{C}$ isotopic ratio and N/C ratio determination. In the case of low $^{12}\text{C}/^{13}\text{C}$ ratio (< 10), these lines are clearly recognized (Fujita 1985), whereas in stars with $^{12}\text{C}/^{13}\text{C} > 20$ both lines are undetectable. Chemical analysis of the expanding envelope (Anupama & Dewangan 2000) also would give useful

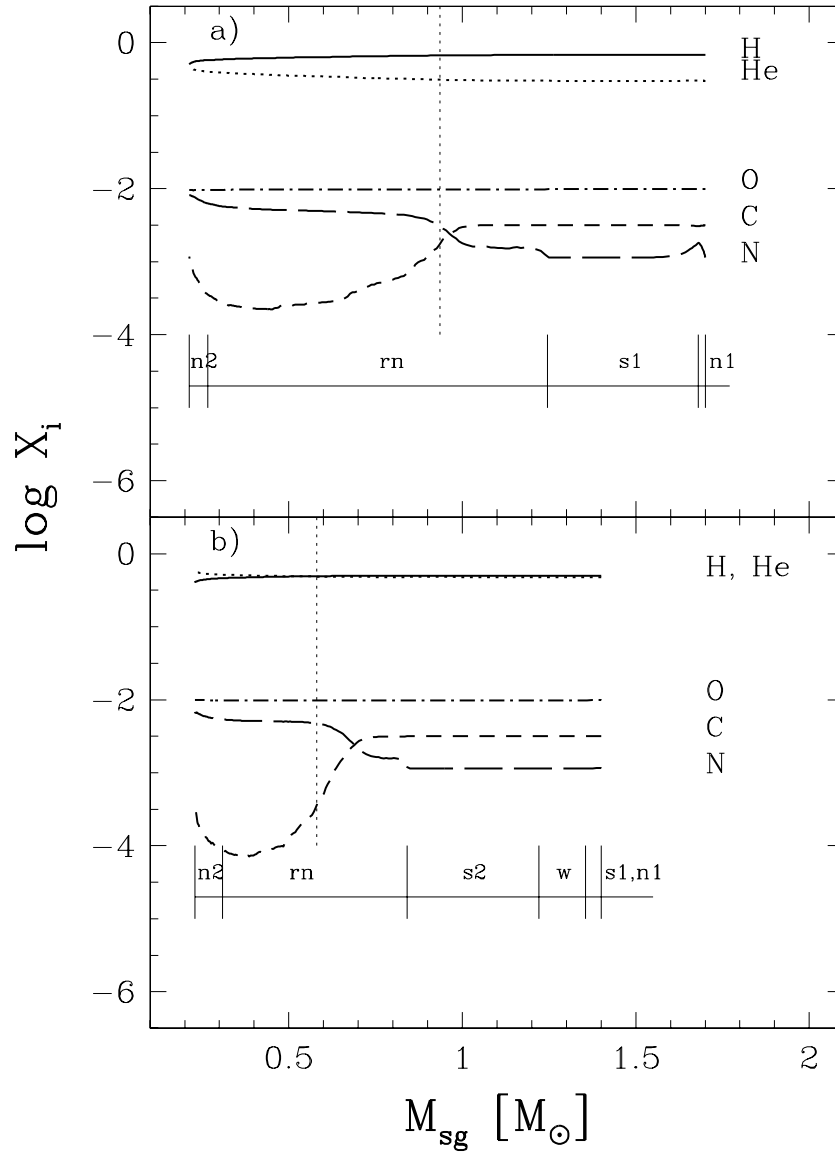


Figure 3: The evolution of the red giant surface abundances (by mass) of H, He, C, N and O as a function of the subgiant mass M_{sg} : upper panel — sequence B, lower panel — sequence C. Vertical thin dashed lines mark the position of subgiant mass for sequences B ($M_{sg} = 0.926 M_{\odot}$) and C ($M_{sg} = 0.603 M_{\odot}$) at $P_{orb} = 1.23$ d, respectively (see Table 2 for more details). The first and second novae phases are marked n1 and n2, respectively; The first and second stable hydrogen shell burning episodes are marked s1 and s2, respectively; and the strong optically thick wind phase is marked w. Systems evolve from right to left. For more explanation see text.

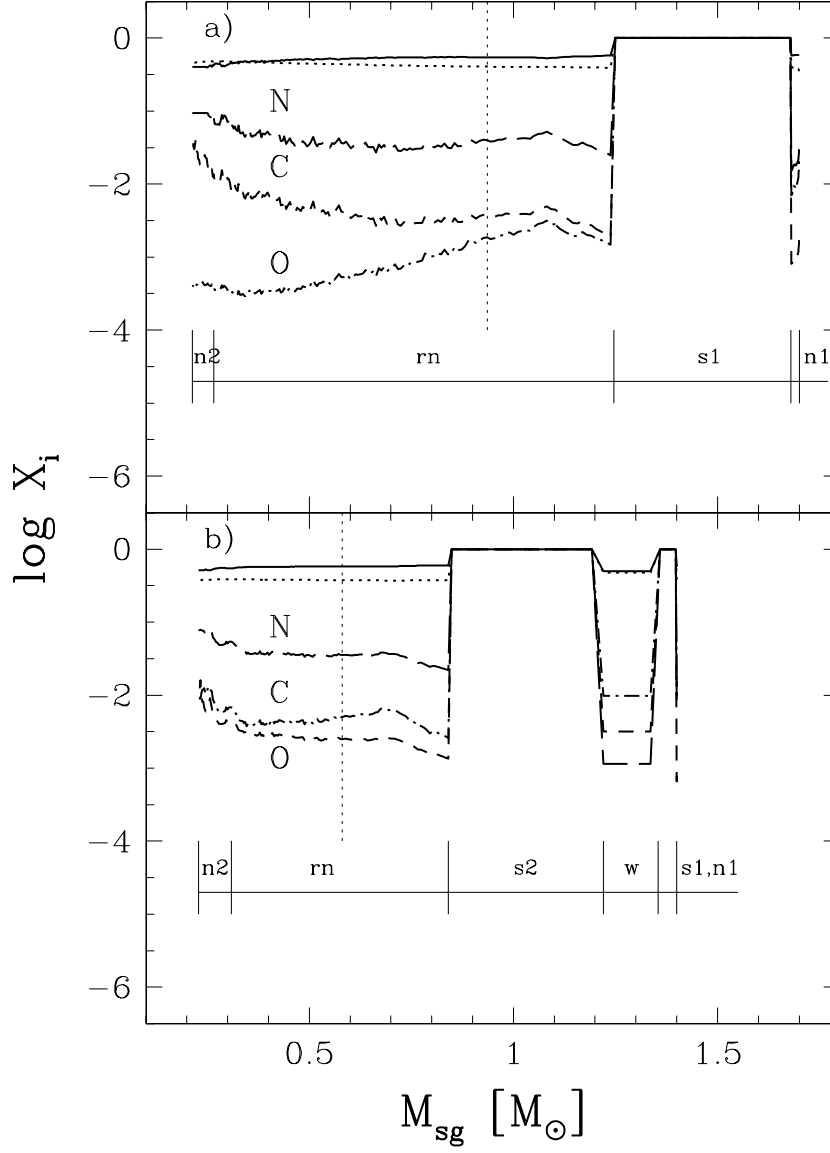


Figure 4: The evolution of ejecta abundances (by mass) of H, He, C, N and O as a function of the subgiant mass M_{sg} : upper panel — sequence B, lower panel — sequence C. Systems evolve from right to left. The various phases are the same as in Fig.3

information, allowing for comparison with theoretical models (see Table 4).

6 Discussion

6.1 Hydrogen-rich vs helium-rich models

Hachisu et al. (1999) proposed a new evolutionary path to SNe Ia formation, in which the companion star is helium-rich. In their model, typical orbital parameters of SNe Ia progenitors are: $M_{\text{wd}} = 1.37 M_{\odot}$, $M_{\text{sg}} \sim 1.3 M_{\odot}$, and $\dot{M}_{\text{sg}} \sim 2 \times 10^{-7} M_{\odot} \text{ yr}^{-1}$. Based on light-curve analysis, Hachisu et al. (2000) also constructed a detailed theoretical model for U Sco. They found that the best fit parameters are: $M_{\text{wd}} \sim 1.37 M_{\odot}$, and $M_{\text{sg}} \sim 1.5 M_{\odot}$ (a range from 0.8 to 2.0 M_{\odot} being acceptable).

However, the helium-enriched model poses a serious problem. Truran et al. (1988) discussed the composition dependence of thermonuclear runaway models for recurrent novae of U Sco-type. They showed that for $M_{\text{wd}} = 1.38 M_{\odot}$, $\dot{M}_{\text{sg}} = 1.5 \times 10^{-8} M_{\odot} \text{ yr}^{-1}$ and $L = 0.1 L_{\odot}$ optically bright outbursts are obtained only for matter with $\text{He}/\text{H} < 1$ by mass. Their results are consistent with our sequences B and C where He/H are equal 0.47 and 0.98, respectively. The large helium content observed in U Sco must then be attributed to helium enrichment from the underlying white dwarf (Priyalnik & Livio 1995).

According to Kato (1996), a supersoft component in UV spectrum is predicted to be observable about 10 days after the outburst. For the hydrogen-rich model ($\text{He}/\text{H}=0.1$) the supersoft X-ray component is expected to rise until ~ 50 days after the outburst to a maximum luminosity of $\sim 3 \times 10^{36} \text{ erg s}^{-1} (d/\text{kpc})^2$. For the helium-rich model ($\text{He}/\text{H} = 2$), the maximum luminosity is reached about 20 days after the optical outburst. The evolution of the X-ray luminosity could therefore give important evidence about the chemical composition of the accreted matter. Unfortunately, only a synoptic soft X-ray detection of U Sco exists, some 19–20 days after outburst (Kahabka et al. 1999).

6.2 The recurrent novae phase

In MS98, a grid of evolutionary sequences for $q_i = 1.25$ and white dwarf initial masses from 0.8 to 1.2 M_{\odot} has been calculated. According to those calculations it is possible to produce a system like U Sco (for Population I chemical composition), but only if the initial white dwarf mass is already very high ($> 1.2 M_{\odot}$). For the model with $M_{\text{wd},i} = 1.2 M_{\odot}$, the system spends less than 1% of its semidetached evolution ($5 \times 10^8 \text{ yr}$) in the recurrent novae phase. For the rest of the time, the system evolves through fast novae and moderately fast novae phases. Our recent calculations for $q_i = 1.25$ show that systems with $M_{\text{wd},i} = 1.3 M_{\odot}$ evolve towards the Chandrasekhar limit (Supernovae Ia). The system spends about 30% of its semidetached evolution ($4.2 \times 10^8 \text{ yr}$) in the recurrent nova phase. In the calculations described here, which begin with higher initial mass ratios and lower-mass white dwarfs, sequences B (hydrogen-rich) and C (helium-rich) both evolve through the recurrent novae phase, and spend in this phase 75% and 65% of their semidetached evolution, respectively (see Table 3). In their final phases of semidetached evolution, massive white dwarfs near the Chandrasekhar limit are formed, but they never exceed this limit.

7 Conclusions

We calculated several evolutionary sequences to reproduce the orbital and physical parameters of the recurrent novae of U Sco-type. The results of these calculations can be summarized as follows:

(1) We find a new evolutionary channel for the formation of the U Sco-type systems. We show that they may form from binaries with a low-mass C-O white dwarf as accretor if $M_{\text{wd},i} < 0.85 M_{\odot}$ and $1.5 < q_i < 2.5$. Such systems evolve through several observable stages: SSS with stable hydrogen burning, strong wind phase, and long-term recurrent nova phase (longer than 10^7 years, Table 3). In the final phase of evolution, massive white dwarfs near the Chandrasekhar mass limit are formed, but they never exceed this limit.

(2) We find that our evolutionary sequence B is able to produce a binary system with parameters similar to U Sco. This model has initial parameters: $M_{\text{sg},i} = 1.7 M_{\odot}$, $M_{\text{wd},i} = 0.85 M_{\odot}$ and $P_i(\text{RLOF}) = 1.61$ d. Based on this evolutionary model, we found that the best fit parameters for U Sco are: $M_{\text{sg}} = 0.94 M_{\odot}$, $M_{\text{wd}} = 1.31 M_{\odot}$, $\log L_{\text{sg}}/L_{\odot} = 0.42$, and $\dot{M}_{\text{sg}} = 3.58 \times 10^{-8} M_{\odot} \text{ yr}^{-1}$ for $P_{\text{orb}} = 1.23056$ d.

ACKNOWLEDGMENTS

This work is partly supported through grants 1 P03D 024 26 from the Ministry of Scientific Research and Information Technology, Poland **and Collaborative Linkage Grant PST.CLG.977383**. JG and EE acknowledge support through Estonian SF grant 4338. EE acknowledges the warm hospitality of the Astronomical Institute “Anton Pannekoek” where part of this work was conducted. While in Netherlands, EE was supported by NWO Spinoza grant 08-0 to E. P. J. van den Heuvel.

References

- [1] Alexander D. R., Ferguson J. W., 1994, ApJ, 437, 879
- [2] Anupama G. C., Dewangan G. C., 2000, AJ, 119, 1359
- [3] Bahcall J. N., Pinsonneault M. H., 1992, Rev. Mod. Phys., 64, 885
- [4] Bahcall J. N., Ulrich R. K., 1988, Rev. Mod. Phys., 60, 297
- [5] Bahcall J. N., Pinsonneault M. H., Wasserburg G. J., 1995, Rev. Mod. Phys., 67, 781
- [6] Barlow M. J. et al., 1981, MNRAS, 195, 61
- [7] Bauschlicher C. W., Langhoff S. R., Taylor P. R., 1988, ApJ, 332, 531
- [8] Cassisi S., Iben I. Jr., Tornambe A., 1998, ApJ, 496, 376
- [9] Caughlan G. R., Fowler W. A., Harris M. J., Zimmerman B. A., 1985, Atom. Data and Nucl. Data Tables, 32, 197
- [10] Caughlan G. R., Fowler W. A., 1988, Atom. Data and Nucl. Data Tables, 40, 283

- [11] Chanan G. A., Nelson J. E., Margon B., 1978, *ApJ*, 226, 963
- [12] De Greve J.-P., 1993, *A&ASS*, 97, 527
- [13] Eggleton P. P., 1983, *ApJ*, 268, 368
- [14] Ergma E., Sarna M. J., 2000, *A&A*, 363, 657
- [15] Fowler W. A., Caughlan G. R., Zimmerman B. A., 1967, *ARA&A*, 5, 525
- [16] Fowler W. A., Caughlan G. R., Zimmerman B. A., 1975, *ARA&A*, 13, 69
- [17] Fujita Y., 1985, in: “Cool Stars with Excesses of Heavy Elements”, eds. M. Jасhek and P. C. Keenan, Dordrecht, Reidel, p. 31
- [18] Hachisu I., Kato M., Nomoto K., 1996, *ApJ*, 470, L97
- [19] Hachisu I., Kato M., Nomoto K., Umeda H., 1999, *ApJ*, 519, 314
- [20] Hachisu I., Kato M., Kato T., Matsumoto K., 2000, *ApJ*, 528, L97
- [21] Harris M. J., Fowler W. A., Caughlan G. R., Zimmerman B. A., 1983, *ARA&A*, 21, 165
- [22] Huebner W. F., Merts A. L., Magee N. H. Jr., Argo M. F., 1977, *Astrophys. Opacity Library*, Los Alamos Scientific Lab. Report No. LA-6760-M
- [23] Iglesias C. A., Rogers F. J., 1996, *ApJ*, 464, 943
- [24] Iijima T., 2002, *A&A*, 387, 1013
- [25] Kahabka P., Hartmann H. W., Parmar A. N., Negueruela I., 1999, *A&A*, 347, L43
- [26] Kato M., 1996, in: “Supersoft X-ray sources”, ed. J. Greiner, *Lecture notes in physics*, vol. 472, Springer, p.15
- [27] Kato M., Hachisu I., 1999, *ApJ*, 513, L41
- [28] Kovetz A., Prialnik D., 1997, *ApJ*, 477, 356 (KP97)
- [29] Kudryashov A. D., Ergma E. V., 1980, *Sov. Astron. Lett.*, 6, 375
- [30] Langer N., Deutschmann A., Wellstein S., Höflich P., 2000, *A&A*, 362, 1046
- [31] Li X.-D., van den Heuvel E. P. L., 1997, *A&A*, 322, L9
- [32] Livio M., Pringle J. E., 1998, *ApJ*, 505, 339
- [33] Livio M., Govarie A., Ritter H., 1991, *A&A*, 246, 84
- [34] Marks P. B., Sarna M. J., Prialnik D., 1997, *MNRAS*, 290, 283
- [35] Marks P. B., Sarna M. J., 1998, *MNRAS*, 301, 699 (MS98)

- [36] Matsumoto K., Kato M., Hachisu I., 2003, PASJ, 55, 297
- [37] Nomoto K., Nariai K., Sugimoto D., 1979, PASP, 31, 287
- [38] Munari U., Zwitter T., Tomov T., Bonifacio P., Selvelli P., Tomasella L., Niedzielski A., Pearce A., 1999, A&A, 347, L39
- [39] Paczyński B., Ziolkowski J. 1967, Acta Astron., 17, 7
- [40] Paczyński B., 1970, Acta Astron., 20, 47
- [41] Pols O. R., Tout C. A., Eggleton P. P., Han Z., 1995, MNRAS, 274, 964
- [42] Prialnik D., Livio M., 1995, PASP, 107, 1201
- [43] Prialnik D., Kovetz A., 1995, ApJ, 445, 789 (PK95)
- [44] Sarna M. J., De Greve J.-P., 1994, A&A, 281, 433
- [45] Sarna M. J., De Greve J.-P., 1996, QJRAS, 37, 11
- [46] Sarna M. J., Marks P. B., Smith R. C., 1996, MNRAS, 279, 88
- [47] Schaefer B.E., 1990, ApJ.,335, L39
- [48] Schaefer B. E., 2004, IAUC, 8278
- [49] Schaefer B. E., Ringwald F. A., 1995, ApJ, 447, L45
- [50] Schneider D. P., Greenstein J. L., 1979, ApJ, 233, 935
- [51] Skumanich A., 1972, ApJ, 171, 565
- [52] Smith M. A., 1979, PASP, 91, 737
- [53] Starrfield S., Sparks W. M., Truran J. W., 1985, ApJ, 291, 136
- [54] Thoroughood T. D., Dhillon V. S., Littlefair S. P., Marsh T. R., Smith D. A., 2001, MNRAS, 327, 1323
- [55] Truran J. W., Livio M., Hayes J., Starrfield S., Sparks W. M., 1988, ApJ, 324, 345
- [56] Warner B., 1995, Cambridge Astrophysics Series, No. 28, Cataclysmic Variable Stars, Cambridge Univ. Press, Cambridge
- [57] Webbink R. F., 1976, ApJ, 209, 829
- [58] Webbink R. F., Livio M., Truran J. W., Orio M., 1987, ApJ, 314, 653
- [59] Williams G., 1983, ApJS, 53, 523
- [60] Williams R. E., Sparks W. M., Gallagher J. S., Ney E. P., Starrfield S. G., Truran J. W., 1981, ApJ, 251, 221
- [61] Ziółkowski J., 1985, Acta Astron., 35, 199